

CONSISTENCY OF INFOMAX ICA DECOMPOSITION OF FUNCTIONAL BRAIN IMAGING DATA

*Jeng-Ren Duann**, *Tzyy-Ping Jung**, *Scott Makeig**, *Terrence J. Sejnowski§**

*Institute for Neural Computation, University of California San Diego, La Jolla CA 92093-0961
§Computational Neurobiology Laboratory, The Salk Institute for Biological Studies, CA 92037, USA

ABSTRACT

Ten spatial infomax ICA decompositions were performed on two fMRI data sets collected from the same subject. The maximally-independent spatial components were then tested across decompositions for one-to-one correspondences. Matching independent component maps by mutual information alone proved ineffective. Matching component map pairs by correlating their z -transformed voxel map weights demonstrated that the top 100 components were stably reproduced in each of the ten decompositions. Infomax ICA therefore provided a stable decomposition of fMRI data into spatially independent components.

1. INTRODUCTION

Independent Component Analysis (ICA) has been successfully applied in a variety of applications including biomedical time series (EEG, ECG, etc.) and images (fMRI, PET, SPECT) [1]. For example, Makeig, et al. [2] applied ICA to separate the multi-channel EEG and found that the basis of the event-related potential, averaged across similar experimental trials, can typically be dissected into several source components accounting for different temporally and functionally distinct EEG processes. This method can better explain the variability of event-related EEG results and can give more complete and consistent results, within and between subjects, than standard methods that measure data features at individual scalp channels [3].

ICA is a relatively model-free blind method that attempts to separate the underlying source

contributions to the data without knowing in advance what the sources are or how they are mixed. Thus, there are no *a priori* suitable statistical models to evaluate the goodness-of-fit of the resultant independent components. For both EEG and fMRI data, the ‘true’ natures of the signal sources are not known. It is therefore difficult to evaluate the performance of ICA for these data precisely.

In their pioneering application of ICA to fMRI data, McKeown et al. [4][5] decomposed one fMRI data set twice, first with random initial weights and the second beginning with the resulting weights from the first decomposition. They then compared the resulting components from the two decompositions using mutual information, selecting a mutual information threshold for detecting highly reproducible components. Meinecke et al. [4] applied a resampling approach to randomly select independent components from an ICA decomposition, then applied ICA to the reassembled dataset to determine which components were reproduced across decompositions. In this paper, we decompose two fMRI data sets, collected from the same subject participating in the same experiment, using infomax ICA and employ a quantitative approach to assess the reproducibility of the decompositions.

We first describe the fMRI data, how we performed the decompositions and how we matched components across different decompositions. We then define the measures by which we evaluated the stability of the decompositions. The resulting component equivalences are then presented. Finally, we discuss the implications of our results for

analysis of fMRI data.

2. METHOD

fMRI Data Set

Two fMRI data sets from one subject who passively viewed reverse checkerboard patterns intermittently presented (for 500 ms or 3000 ms every 30 sec, as described in Duann et al. [7]) were used for multiple ICA decompositions to evaluate the stability of ICA results. These data each consisted of 5 slices of 64×64 functional brain images with an inter-scan interval (TR) of 0.5 sec, collected using a 3-Tesla research scanner at the Taipei Veterans General Hospital, Taiwan.

Data Analysis

Before image preprocessing, 5-6 corrupt ('dummy') scans were removed from the beginning of the fMRI data. Then, the data were subjected to slice timing adjustment to minimize inhomogeneities arising from acquisition of the five image planes at different times. We then removed voxels outside the brain volume to reduce the data size for ICA training and also to eliminate possible sources of machine noise arising from susceptibility differences between air and brain tissues. The fMRI time series were then transposed to form a matrix with dimension $N \times V$, where N is the number of scans (in our case, $N=600$) and V , the number of voxels remaining after image preprocessing (here $V=4047$). The fMRI time series matrix was then subjected to infomax ICA decomposition [8] to obtain an unmixing matrix. Multiplying the data by this matrix produced the estimated component maps and time courses. Since the number of voxel time courses decomposed (~9000) was not sufficient to derive a full (600×600) unmixing matrix, the dimensionality of the data was reduced to 100 by PCA before training. The unmixing weights were initialized with the unity matrix. To assure the full convergence of ICA training, the number of training steps was increased to 2048. For further details, see Duann et al. [7].

Multiple ICA Decompositions

To evaluate the stability and consistency of infomax decomposition, each of the preprocessed fMRI data sets was decomposed by infomax ICA ten times using the same initial conditions and training parameters. Variability in the output of the infomax algorithm [8] is induced by the random shuffling of the training (voxel) data order before each training step. Next, the activation matrices containing the spatial component maps were obtained by

$$\mathbf{u}^i = \mathbf{W}^i \times \mathbf{x} \quad (1)$$

where \mathbf{u}^i are the 'activation' map weights of the i^{th} decomposition, \mathbf{W}^i is the inverse matrix of the i^{th} decomposition of the training data set \mathbf{x} . The activations were transformed to z values by

$$z_{j,k}^i = \frac{u_{j,k}^i - \frac{1}{K} \sum_k u_{j,k}^i}{\sqrt{\sum_k \left(u_{j,k}^i - \frac{1}{K} \sum_k u_{j,k}^i \right)^2}} \quad (2)$$

where i is the decomposition index, j the number of components, and k the number of voxels; K is the total number of voxels in the training data set, and $u_{j,k}^i$ and $z_{j,k}^i$ are the activation weights and the z value of k^{th} voxel contributed by the j^{th} component in the i^{th} decomposition, respectively. Assessments of how well component classes were matched and their stability were performed on the z-transformed component maps.

Matching Component Pair Assignments

The first question was whether for each component in any one of the decompositions, it was possible to identify a single best-matching component in each of the other decompositions. To determine this, we first needed to find best-matching component pairs for pairs of decompositions. We tried three different similarity measures: mutual information, cross correlation, and cross correlation with mutual information weighting of the component maps weights. The measure of mutual information we used was:

$$MI(x, y) = 2 * [H(x) + H(y) - H(x, y)] / [H(x) + H(y)]$$

$$H(x) = - \sum_{i=1}^N p(x_i) \ln(p(x_i)) \quad (3)$$

where MI is normalized mutual information, $H(x)$ is the entropy of random variable x (map weights), and the entropy is derived from its histogram with N bins. For N , we used the cube root of the number of voxels involved in the ICA training. To eliminate fluctuations created by the entropy of the weights used in the estimation, we normalized mutual information (as above) by dividing it by the sum of the weight entropies.

For each measure, best matching component pairs were assigned by repeatedly selecting, without substitution, the most similar pair of remaining components. Cross correlation coefficients between best-matching component map pairs proved to be quite high, essentially separating the 10×100 components into 100 equivalence classes consisting of 10 components, one from each decomposition. To better differentiate best and worst component classes, we investigated a joint component pair similarity measure, the product of cross correlation and mutual information.

Evaluating the Stability of ICA results

To assess the stability of the decompositions, we then computed the standard deviation of the z -transformed map weights across each component equivalence class, as well as the cross correlations of the matching component time courses. The first measure was obtained by

$$A_{STD} = \sum_{k \in \text{window}} \left[\sum_i \left(\frac{(z_k^i - \bar{z}_k)^2}{|\bar{z}_k|} \right)^{1/2} \right] \quad (4)$$

where z_k^i is the weight at voxel k in the i th decomposition and \bar{z}_k is the mean weight at the same voxel k across the ten decompositions. We computed A_{STD} , the standard deviation of map weights (in z values) across decompositions, within a window of 50 voxels moved through the voxel data (sorted by z value) in 25-voxel steps.

As a second index of component stability, we calculated the mean cross correlation between time courses of nine component pairs in each equivalence class (e.g. the first decomposition vs. the others).

3. RESULTS

Fig. 1 shows the results of matching component pairs between first and all other nine decompositions (for the first data set) using the three different similarity measures (top row, mutual information; bottom row, cross correlation). The left panels show the best-matching component pair assignments. Here, the component numbers (ordered by the infomax algorithm in reverse order of data variance accounted for) are color-coded (blue=#1 to red=#100). The first row of each figure shows the components in the first decomposition in their original component order (from 1 to 100). The color (assigned using the same convention described above) in other rows of the figure indicates the best-matching component number in the other nine decompositions. For example, component #100 in the fifth decomposition is assigned to component #25 in the first decomposition (red arrow, Fig. 1a), the best-matching component by mutual information. Fig. 1 shows clearly that nearly all best-matching component pairs, by mutual information, were closely matched in amplitude rank (i.e., component number). Using cross correlation, with or without weighting by mutual information, produced matches with more component-number adjustments ($a_i \leftrightarrow b_j$ where $i \neq j$).

Fig. 1 (top right) shows the mutual information measure for the best-matching pairs. For all nine comparisons, the mutual information trends contain an abrupt drop (“knee point”) between component pairs 20 and 40. Above this knee point, the mutual information between matching components is close to zero. For example, for the comparison between decompositions 1 and 2, MI values for later pairs were between 0.0011 and 0.0018. Based on this measure [5, 6], one might guess that only 20 to

40 of the 100 independent components were reproduced in all decompositions. However, the results of matching based on absolute correlations gave quite a different result (Fig. 1c and 1d), which showed that all 100 component maps were faithfully reproduced in every decompositions (the minimum map weight correlation was 0.925, Fig. 1d). Cross correlation weighted by mutual information found the same best-matching pairs as matching by correlation alone.

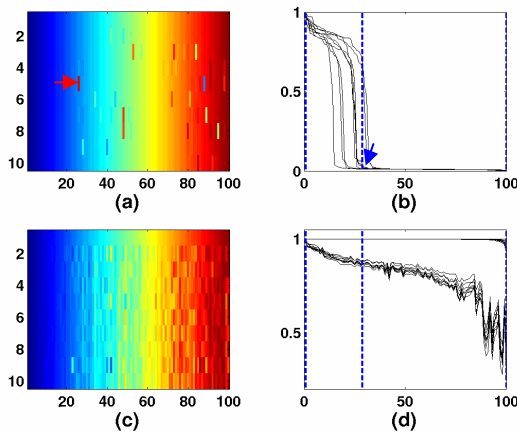


Fig. 1 Best-matching components obtained from multiple decompositions. (a) Indices of the best-matching component pairs from the first decomposition and the others, as found by maximum mutual information. Component indices are color-coded (component, 1 blue; component 100, red as in the top row). (b) Mutual information between the best-matching components sorted by its magnitude. The nine traces reflect component pairings between the first decomposition and the others. Three vertical dotted lines indicate respectively the best matching component pair (1^{st}), the distribution “knee point” (29^{th}), and the least well-matching component pair (100^{th}) for decompositions 1 and 2. (c) The component pair assignments from based on maximum absolute correlation coefficients.. (Using correlations multiplied by MI gave identical component pair assignments). (d) Correlation coefficients between the matching component pairs shown in (c). Upper traces: Correlation coefficients; lower traces: correlations times mutual information, both sorted by mean absolute correlation.

Fig. 2 shows, for each of the three similarity measures, scatter plots of the component map weights for the first most, twenty-ninth (at the knee point indicated by blue arrow in Fig. 1b)

and least most (100^{th}) well-matching pairs from the first and second decompositions (indicated by three vertical dotted lines in Fig. 1b and 1d).

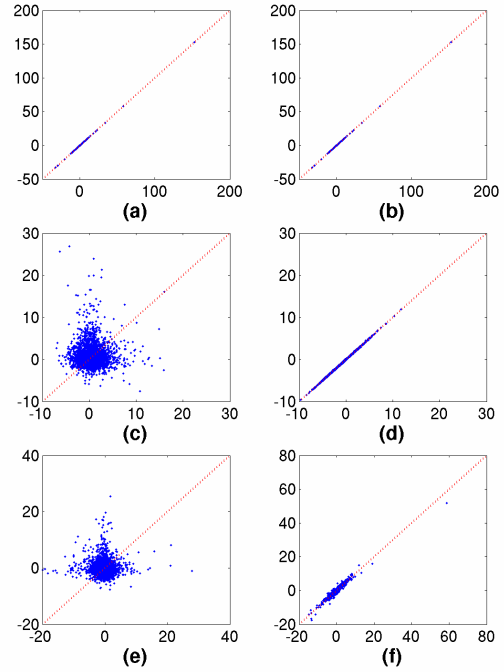


Fig. 2 Comparisons between best-matching component pairs found using mutual information (a, c, and e, left) and absolute cross correlation weighted by mutual information (b, d and f, right).

In Fig. 2, the scatter plots of map weights of the two corresponding components distinctly follow $y=x$ line ($r=1.00$, $MI=0.9714$ in Fig. 2a and 2b). Fig. 2c shows the scatter plot of the activations of corresponding components of the component pair obtained by maximum mutual information at the ‘knee point’ indicated by a blue arrow in Fig. 1b. The voxel data do not adhere to the $y=x$ line ($MI=0.0018$). For comparison purposed, in Fig. 2d, we show the scatter plot of matching components of 29^{th} component pair obtained using method of absolute cross correlation weighted by mutual information. These data follow fall on the diagonal line ($CC=0.9994$ and $MI=0.8685$). The distribution of the 29^{th} component pair data ($MI=0.8685$) is wider than that of the first pair ($MI=0.9714$), although it may be difficult to

distinguish the two pairs correlation coefficient alone ($CC=1.00$ vs. $CC=0.9994$).

Although the voxel weights of the least well-matching component pair by mutual information alone (Fig. 2e) do not follow $y=x$ line ($MI=0.0011$), the least well-matched pair by cross correlation (with or without weighting by mutual information) closely follows the $y=x$ line ($CC=0.9820$, $MI=0.2214$, Fig. 2f). Here mutual information weighting ($MI=0.8685$ vs. $MI=0.2214$ in Figs. 2d and 2f) appears more sensitive to differences than correlation coefficients alone ($CC=0.9994$ vs. $CC=0.9820$).

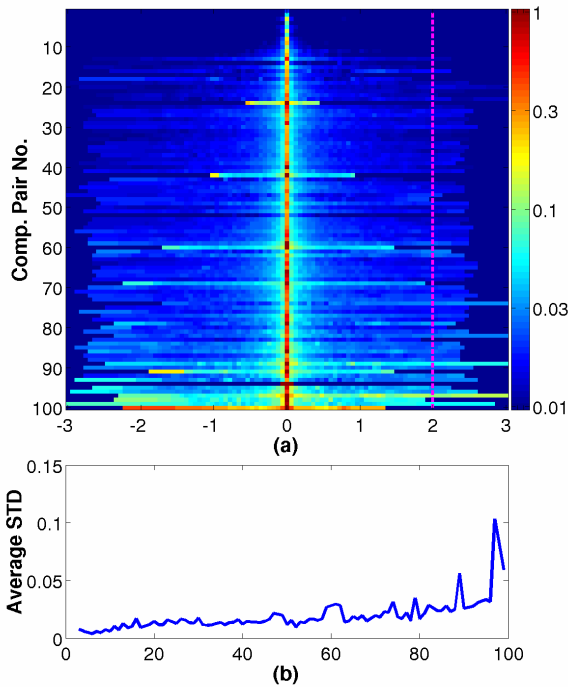


Fig. 3 (Top panel) Color-coded standard deviations (across ten decompositions) of voxel component map weights for fifty-voxel windows moved across the z -value range (abscissa). Note that the peaks around zero in these plots are introduced by normalization of near-zero z values in Eq. (3). (Bottom panel) Standard deviations (ordinate) within the fifty-voxel window centered at $z = 2$ (dotted line in top panel) for the 100 best-matching component classes reverse-ordered (abscissa) by map-weight correlation.

Fig. 3 shows the standard deviation of voxel weights (from Eq. 4) across the 10

decompositions as a function of median z value, computed for a 50-voxel window moving in a 25-voxel step through the brain voxels sorted in order of increasing mean z values. We consider the tails of the z -weight distribution, e.g. with weights $z > 2$, to be the voxels defining component's region of activity (ROA) [7]. Fig. 3b shows the standard deviation of map weights in the voxel window centered at $z = 2$ (vertical red line in Fig. 3a). The ROA-boundary weights are most stable for the overall best-matching 10 component classes, and appear increasingly less stable for component classes 50-100; however, these deviations can be negligible.

We also investigated the similarity of the BOLD-signal time courses of matching component pairs from different decompositions. The absolute correlations were very high (0.94 ~ 1.0). The same procedure applied to the second data set from the same subject produced equivalent results.

4. DISCUSSION

Correctly determining the best-matching component pairs is an important issue in evaluating the stability of ICA decompositions. These results suggest matching component pairs using maximum correlation, with or without mutual information weighting, is a straightforward and effective method for determining best-matching component classes from multiple ICA decompositions of the same data. For these data, even the least best-matching component pairs exhibited strong stability. Our results do not support the claim of McKeown [5] who proposed that mutual information is a useful method for discarding unreliable components, using the "knee" of the mutual information distribution. Although we also found a 'knee' in the component distribution, correlating z -transformed map weights for the same data demonstrated that the mutual information method produced clearly sub-optimum component pair assignments (Fig. 2). In fact, component-pair matching by map correlations

demonstrated that every component in each decomposition had a well-matching counterpart in every other decomposition. Therefore, components not well-matched by mutual information were not necessarily “noisy” components to be rejected from further analysis. Thus, our results show that with correct correlation-based component matching, the components obtained from repeated infomax ICA decompositions are highly stable and consistent, with weights that vary little across decompositions. The time courses of best-matching components are also retained across decompositions.

However, automatic categorization of fMRI components as task-related, non-task related or artifact, often of interest to fMRI researchers, is a more difficult problem. Detailed examination of the best-reproduced ten components (Fig. 3, lower left) showed these to include three components most probably arising from subject movement and three others from arterial pulsations. Two others exhibited slow drifts of unknown origin. Only two of the ten accounted for task- and stimulus-related BOLD activity (stimulus-related visual and scanner-noise auditory response areas).

We have recently developed an ICA component browser application, FMRLAB, which allows experimenters to quickly compute and then browse through properties of the independent components of their data, marking some for rejection as artifact and/or selecting others for further analysis. FMRLAB runs on several platforms in the MATLAB (The Mathworks, Inc.) environment, and is freely available for non-commercial use via our web site [9].

5. CONCLUSIONS

Assessing the consistency or stability of ICA decomposition of fMRI data is an important issue for interpreting the results. Here, we utilized multiple decompositions of the same fMRI data sets into spatially independent

components to measure the stability of infomax ICA. The infomax algorithm [8] never failed to converge to a stable solution. Moreover, measures of component voxel weight and time courses showed the repeated infomax ICA decompositions were extremely stable. These promising results need to be further tested using fMRI datasets from different experimental paradigms and using more general resampling methods [6].

6. REFERENCES

- [1] Jung, T.-P., Makeig, S., McKeown, M. J., Bell, A. J., Lee, T.-W., Sejnowski, T. J., "Imaging brain dynamics using independent component analysis." *Proceedings of the IEEE*, 89(7): 1107-22 (2001).
- [2] Makeig, S., Bell, A.J., Jung, T.-P. and Sejnowski, T.J., "Independent component analysis of electroencephalographic data," In: D. Touretzky, M. Mozer and M. Hasselmo (Eds). *Advances in Neural Information Processing Systems 8*:145-151 MIT Press, Cambridge, MA, 1996.
- [3] Makeig, S., Westerfield, M., Jung, T.-P., Enghoff, S., Townsend, J., Courchesne E, Sejnowski T.J. Dynamic brain sources of visual evoked responses. *Science* 295: 690-694 (2002).
- [4] McKeown, M.J., Varadarajan, V., Huettel, S. & McCarthy, G. Deterministic and stochastic features of fMRI data: implications for analysis of event-related experiments. *Journal of Neuroscience Methods* 118: 103-113 (2002).
- [5] McKeown, M.J. Deterministic and stochastic features of fMRI data: Implications for data averaging. in *Exploratory Analysis and Data Modeling in Functional Neuroimaging* (Eds Sommer, F.T. & Wichert, A.) 63 (The MIT Press, Cambridge, Massachusetts, 2002).
- [6] Meinecke, F., Ziehe, A., Kawanabe, M. & Muller, K.-R. Assessing reliability of ICA projections - A resampling approach. in *3rd International Conference on Independent Component Analysis on Signal Separation* 74-79, San Diego, 2000).
- [7] Duann, J.R., Jung, T.P., Kuo, W.J., Yeh, T.C., Makeig, S., Hsieh, J.C. and Sejnowski, T.J., Single-trial variability in event-related BOLD signal, *Neuroimage*, 15: 823-835 (2002)
- [8] Makeig, S. et al., World Wide Web publication (1997), Now available from <http://sccn.ucsd.edu/fmrlab/>.
- [9] Duann, J-R., Jung, T-P. and Makeig, S. FMRLAB: Matlab software for independent component analysis of fMRI data. World Wide Web publication (2003), available from <http://sccn.ucsd.edu/fmrlab/>.

Acknowledgments: This work was supported by the National Institutes of Health USA, the Howard Hughes Medical Institute, and The Swartz Foundation.